Applied Physics Letters PERSPECTIVE pubs.aip.org/aip/apl

Perspective on phase change composites in high-efficiency solar-thermal energy storage

Cite as: Appl. Phys. Lett. **126**, 050501 (2025); doi: 10.1063/5.0248794
Submitted: 13 November 2024 · Accepted: 21 January 2025 ·
Published Online: 3 February 2025

View Online Export Citation CrossMark

Zhizhao Mai,[1] Kaijie You,[1] Jianyong Chen,[1] Xinxin Sheng,[1,2,a)] and Ying Chen[1,a)]

AFFILIATIONS

[1]Guangdong Provincial Key Laboratory of Functional Soft Condensed Matter, School of Materials and Energy, Guangdong University of Technology, Guangzhou 510006, China
[2]Department of Polymeric Materials and Engineering, School of Materials and Energy, Guangdong University of Technology, Guangzhou 510006, China

[a)]**Authors to whom correspondence should be addressed:** xinxin.sheng@gdut.edu.cn and chenying@gdut.edu.cn

ABSTRACT

To clarify future research directions, this study first analyzes the heat transfer process of solar-thermal conversion and then reviews solar-thermal phase change composites for high-efficiency harnessing solar energy. The focus is on enhancing heat absorption and conduction while aiming to suppress reflection, radiation, and convection. Most advancements have concentrated on improving absorption and thermal conductivity, while reducing the aforementioned unfavorable processes remains less explored. In the current research, the best results show that the solar-thermal conversion efficiency has approached the theoretical limit (100%), and a typical thermal conductivity has reached 33.5 W/(m·K). However, further enhancement of the absorption and conduction remains a challenge, highlighting the need for structural modifications and grafting. Other factors hindering conversion efficiency have received limited attention and warrant further in-depth investigation, with the potential to reduce reliance on fossil fuels and contribute to environmental sustainability.

I. INTRODUCTION

Solar-thermal conversion, which collects solar radiation and directly converts it into heat, is considered one of the most reliable methods for effectively utilizing abundant solar energy. It not only offers advantages such as cost efficiency, simple equipment, and inexhaustibility, but also has significant potential for energy saving and reducing carbon emissions.[1,2] The study[3] explored the impact of solar-thermal utilization on China's top 10 industrial sectors, predicting a reduction of 98.22×10^6 tons of CO_2 emissions and 39.40×10^6 tons of coal consumption by 2020. Another study[4] concluded that integrating solar-thermal conversion into German enterprises could meet approximately 3.4% or 16 TWh of the heating demand, suggesting that solar-thermal has the potential to significantly replace parts of fossil fuel consumption in human society. However, solar-thermal conversion faces challenges of temporal and spatial mismatches in supply and utilization, requiring thermal energy storage to address this inherent discrepancy. Compared to sensible thermal energy storage and thermochemical thermal energy storage, latent heat thermal energy storage with phase change material (PCM) provides a higher energy storage density and the ability to maintain nearly constant operating temperatures, respectively, positioning latent heat thermal energy storage as an emerging solution for solar-thermal energy storage.[5] In traditional solar-thermal conversion and storage systems, solar collectors and heat exchangers for PCM charging are two essential yet separate devices.[6,7] To overcome challenges, such as complex components, extensive pipelines, and low system efficiency, significant efforts have been made to integrate solar-thermal fillers with PCM for high-efficiency direct solar-thermal conversion and storage. Given that the heat collection approach of the obtained phase change composites (PCC) differs from traditional ones, improving the heat collection capability of PCC has become a key focus of research. This work analyzes the heat transfer behavior during solar-thermal conversion and reviews the current studies in the field. It also highlights the existing challenges and outlines directions for future research. This study provides guidance for improving solar-thermal conversion efficiency, with the goal of further utilizing renewable solar energy and reducing environmental pollution.

II. THE STATUS OF SOLAR-THERMAL CONVERSION AND ENERGY STORAGE

The solar-thermal energy conversion and storage processes in PCC consist of two stages: first, solar radiation energy is converted

into thermal energy on the surface of the PCC, and then, the heat was transferred to the PCM inside for storage. On the first stage, when sunlight is projected onto the surface, three phenomena may occur, including absorption, reflection, and transmission. According to the law of energy conservation, the sum of absorbed, reflected, and transmitted energy equals the incident energy,[6] as illustrated in Fig. 1. When radiant energy enters the surface of a solid or liquid, it is fully absorbed over a very short distance. For conductors like metal, this distance is typically around 1 μm, while for the most of non-conductive materials, it is less than 1 mm. In practical applications, the thickness of PCC generally exceeds this distance, which means the transmission phenomenon in the PCC can be neglected, leaving only reflection and absorption. Enhancing the absorption rate and reducing the reflection rate has become the first trend for improving solar-thermal conversion capacity. On the second stage, the converted thermal energy on the surface can be transferred through three pathways: radiative heat loss to the sky, convective heat loss to the surrounding air, and heat transfer into the PCC by heat conduction. Heat loss to the sky and air causes substantial heat loss from the PCC surface due to its temperature is significantly higher than the surrounding's temperature, making it essential to minimize these losses. So, the second significant trend for solar-thermal PCC is to minimize heat losses and to enhance heat transfer within the PCC. The current research on developing high-efficiency solar-thermal PCC primarily targets two aspects: enhancing the absorption rate and improving heat transfer within the PCC.

A. The status of enhancing the absorption rate

The standard solar spectrum includes the ultraviolet (UV) range (300–380 nm), visible light range (380–760 nm), and near-infrared range (760–2500 nm), with power distribution on earth's surface approximately 3% in UV, 45% in visible, and 52% in near-infrared.[8] The pure PCM has an inherently low sunlight absorption rate, which is unfavorable for solar-thermal conversion. To maximize the sunlight absorption rate of materials, researchers have proposed the full-spectrum absorption theory of solar energy, incorporating various fillers to absorb as many wavelengths of sunlight as possible. Carbon-based,[9–13] MXene-based,[14–16] metallic-based,[17,18] semiconductor-based,[19–21] and organic polymers-based[22–24] are the main categories currently used to enhance sunlight absorption rates.

Carbon-based materials, spanning from zero-dimensional (0D) to three-dimensional (3D) structures, such as carbon dots,[25] carbon black,[26] carbon nanotubes (CNTs),[27] graphene,[28] expanded graphite,[6] biomass-derived carbon,[29] and their derived carbon aerogels,[30–33] have been widely used as solar-thermal conversion fillers in PCC to fully leverage their exceptional absorption across the whole solar spectrum. In contrast to metallic and semiconductor materials, carbon-based materials, leveraging conjugate and hyperconjugate effects, offer a broader spectral absorption range and superior absorption and conversion efficiency, driving their widespread use in recent years.[34] Sun *et al.*[35] strengthened the graphene aerogel framework with polyvinylidene fluoride-hexafluoropropylene, achieving 95.98% solar-thermal conversion efficiency.

MXene-based materials, a new class of two-dimensional (2D) materials composed of transition metal carbides and nitrides, are promising solar-thermal fillers. With high thermal conductivity and strong localized surface plasmon resonance (LSPR) for harvesting visible and near-infrared sunlight, MXenes are highly suited for solar-thermal energy conversion.[34,36] Mo *et al.*[37] developed a novel PCC supported by $Ti_3C_2T_x$@PVA foam, achieving a photothermal conversion efficiency of 96.5%. Despite its impressive solar-thermal conversion capability, MXene still faces challenges such as high production costs and difficulties in large-scale manufacturing.

Metallic-based materials are ideal for solar-thermal energy conversion due to their excellent light absorption and high thermal

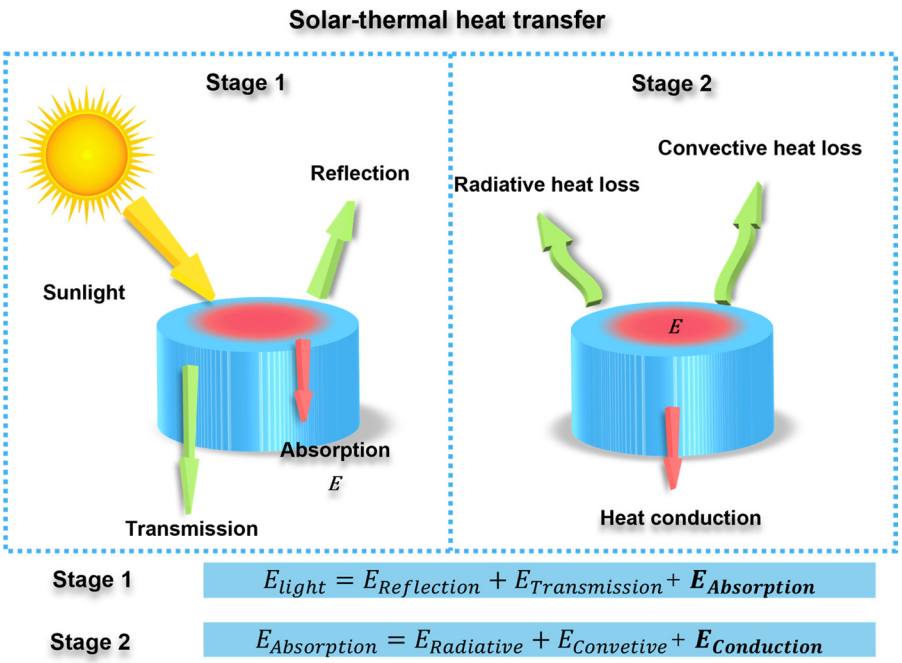

FIG. 1. Schematic diagram of the heat transfer in solar-thermal PCC.

conductivity. The solar-thermal conversion of metallic-based PCC relies on the surface plasmon resonance (SPR) or LSPR effect, enabling infrared light absorption for efficient conversion.[34] Guo *et al.*[38] developed a honeycomb-like 3D porous Cu skeleton, achieving 89.2% solar-thermal conversion efficiency. However, the absorption range of metallic-based materials is typically limited to one or a few LSPR wavelengths, requiring structural engineering to enhance efficiency.

Semiconductor materials, offering unique near-infrared light absorption and tunable spectra, enable efficient solar-thermal conversion. Some rely on nonradiative relaxation, while others, doped with metal ions or oxides, combine LSPR and nonradiative effects.[39] Xiong *et al.*[20] reached 92.9% efficiency with CuS nanoparticles and solid–solid PCM polyurethane.

As organic polymers, polypyrrole demonstrates excellent solar-thermal conversion capacity due to broadband light absorption property, and polydopamine shows strong light absorption capabilities across the UV, visible, and near-infrared spectra, making them outstanding materials for solar-thermal conversion in PCC.[40] Yuan *et al.*[41] constructed phytic acid/dopamine-decorated delignified wood to encapsulate PCM, with the solar-thermal conversion efficiency reached 90.5%. Despite their strong performance, research on semiconductor-based and organic polymer-enabled solar-thermal PCC remains limited.

Although single-component PCC have shown exceptional solar-thermal conversion capacity, their efficiency has not yet reached the theoretical limit. Additionally, most solar-thermal tests show heat collection temperatures between 65 and 80 °C, rarely exceeding 90 °C. Therefore, researchers are working to combine multi-component solar-thermal fillers with PCC to achieve a higher conversion efficiency and temperature. Chen *et al.*[42] synthesized a wood aerogel (nanowood) supporting PEG with a MXene hybrid, with a remarkable solar-thermal conversion efficiency of 98.58% at 10% MXene content. Compared to single-component PCC, multi-component PCC show slight improvements in conversion efficiency, approaching the theoretical limit, with higher surface temperatures. However, the surface temperature still struggles to exceed 100 °C. This may suggest that the current research has pushed solar-thermal absorption efficiency toward the theoretical limit (100%). Future studies aiming to further improve solar-thermal conversion capacity may focus on structural engineering.

This section provides a comprehensive review of solar-thermal conversion PCC, focusing on enhancing their solar-thermal conversion capacity. Scholars have systematically studied various types of solar-thermal materials, showing that nearly all fillers achieve over 90% solar-thermal efficiency. To our knowledge, solar-thermal conversion efficiencies of various single-component PCC, from highest to lowest, are as follows: MXene (above 95%), semiconductors and carbon-based materials (above 90%), and metals and organic fillers (around 90%). To further enhance solar-thermal conversion efficiency, research has combined multi-component solar-thermal materials, pushing the conversion efficiency close to the theoretical limit (100%). However, PCC heat collection temperatures rarely exceed 90 °C, limiting broader applications. Achieving higher temperatures may require reducing PCM content or incorporating structural modifications.

B. The status of enhancing thermal conduction

Given that the primary heat transfer mechanism within the PCC is heat conduction, enhancing its thermal conductivity is essential for improving heat transfer from the surface to the core. For conductive PCM, such as metals, heat transfer is primarily governed by electron transport.[43–45] However, in most inorganic nonmetals, electrons are bound within the ionic lattice, with very few free electrons available to act as heat carriers. As a result, in nonmetallic PCM, such as paraffin and sugar alcohol, heat conduction occurs mainly through lattice vibrations. These vibrations generate elastic sound waves, the energy of which is quantized into phonons, the primary heat carriers in these PCM. In general, stronger phonon diffusion within a material leads to a higher thermal conductivity. Enhancing the thermal conductivity of PCC primarily involves increasing the effective phonon transmission rate.

The transport of phonons in composites is primarily governed by three factors: phonon velocity, specific heat capacity, and mean free path. Aside from the factors mentioned above, phonon transmission within PCC is influenced by various parameters, such as temperature, atomic mass, density, and binding energy. Phonon scattering is the primary mechanism leading to reduced phonon diffusion in PCC.[44] By altering or even reversing the direction of energy transfer, phonon scattering significantly reduces the phonon mean free path, thereby becoming a major constraint on the thermal conductivity of PCC.

The incorporation of high thermal conductivity fillers is a common approach to enhancing the thermal conductivity of PCM. Currently, two primary strategies are used to integrate fillers with PCM. The first method directly disperses fillers into PCM for improving its thermal conductivity. However, within the composite, the fillers are isolated from each other by the PCM, resulting in a "discrete island" distribution. The continuous phase remains the PCM, which inherently has low thermal conductivity.[46] Additionally, the random dispersion of fillers introduces numerous filler–filler and filler–PCM contact interfaces, leading to significant phonon scattering, increased interfacial thermal resistance, and impaired cross-interface heat transfer. Meanwhile, most commonly used fillers [one-dimensional (1D) and 2D] exhibit anisotropic thermal conductivity. For example, the in-plane thermal conductivity of 2D fillers is approximately two orders of magnitude higher than their through-plane conductivity. Simple blending method cannot optimize the orientation of 2D fillers, resulting in low utilization of their in-plane high thermal conductivity. This limitation hinders further enhancement of the composite's thermal conductivity. As a result, constructing a conductive percolation network requires high filler loading, which may reduce the phase change enthalpy of the PCC.

The second method focuses on creating a thermal conduction network within the PCM, especially oriented thermal pathways, to fully leverage the anisotropic thermal conductivity characteristics of fillers. This approach can reduce phonon scattering and interfacial thermal resistance, thereby achieving high thermal conductivity with a low filler content. In constructing the thermal conduction network, it is also important to minimize the introduction of impurities and molecular defects, along with improving crystallinity and orientation to facilitate the thermal conductivity.[47,48] The oriented structure is typically achieved by applying external forces,[49] such as temperature fields, electric fields, or magnetic fields, to align the fillers and construct a 3D network, thereby forming highly ordered directional structures to enhance the phonon mean free path. Theoretically, the thermal conductivity efficiency of fillers follows the trend of $3D > 2D > 1D$, as the total interfacial area decreases with the increasing size of the

nanofillers. Therefore, many studies have constructed 3D thermal conduction networks and explored their impact on thermal conductivity. Li *et al.*[6] tailored thermal transports by aligning self-assembled large-size reticulated graphite nanoplatelets inside PCM with a thermal conductivity of up to 33.5 W/(m·K) at loading below 25 wt. %. To our knowledge, this represents a typical high thermal conductivity PCC in current research.

Further studies have shown that the mismatch between fillers and PCM is a major source of phonon scattering. Compared to forming a 3D thermal conduction network solely through van der Waals interactions, grafting functional groups onto the fillers can effectively improve their compatibility and interaction with the PCM, while also enhancing the interfacial bonding strength between the fillers and the PCM. This may lead to an order-of-magnitude reduction in the interfacial thermal resistance between adjacent conductive fillers. Researches have also demonstrated that increasing the graft chain length and graft density[50,51] of the functional groups on the filler surface can actively contribute to reducing interfacial thermal resistance. Li *et al.*[52] prepared PCC using paraffin and grafted CNTs, achieving a thermal conductivity of 0.7903 W/(m·K) at 4 wt. % CNTs. Grafted CNTs with longer carbon chains showed a higher thermal conductivity and a lower interfacial thermal resistance compared to ungrafted CNTs, due to improved compatibility with paraffin. Although grafted fillers have not achieved particularly notable results in PCC research, they have demonstrated exceptionally high thermal conductivity in other composite systems. Yan *et al.*[50] introduced a rapid, high-yield method for producing exfoliated boron nitride nanosheets (BNNS), achieving a record high aspect ratio of ≈1500 with minimal defects. This approach has been utilized to fabricate a foldable, electrically insulating film by combining BNNS with a poly(vinyl alcohol) (PVA) matrix through filtration. The resulting film demonstrates an impressive in-plane thermal conductivity of 67.6 W/(m·K) at a BNNS loading of 83 wt. %. Enhancing thermal conductivity through grafting to form chemical bonds has emerged as a promising direction for future advancements in thermal conductivity improvement. However, grafting has its drawbacks. Although grafting improves the interfacial bonding strength between the filler and PCM, it can also result in a reduction in the intrinsic thermal conductivity of the filler. These two effects are in competition, representing a common limitation of the grafting method. The decrease in the intrinsic thermal conductivity of the filler after grafting is primarily due to the introduction of numerous defects into the crystal structure by the grafted functional groups, which disrupt the crystal structure of the fillers and increase phonon scattering. Therefore, it is preferable to graft the functional groups at the edges of the fillers to optimize the phonon transport at the filler–PCM interface, thereby further enhancing the thermal conductivity of the composite material.

This section primarily reviews strategies for enhancing the thermal conductivity of PCC, summarizing the heat transfer mechanisms and improvement approaches. Phonon scattering is a critical factor affecting thermal conductivity, and constructing oriented thermal conduction pathways within PCC proves to be an effective solution, achieving levels up to 33.5 W/(m·K) at a filler loading below 25 wt. %. However, it is still modest compared to copper's thermal conductivity [approximately 390 W/(m·K)], showing an order-of-magnitude gap. Subsequent studies identified interfacial thermal resistance between fillers and PCM as the main source of phonon scattering. Grafting functional groups onto fillers has shown potential in improving compatibility and interaction with PCM, enhancing interfacial bonding strength, and has been validated in thermal interface material research, though its application in solar-thermal PCC studies remains limited. Further research works lie in understanding phonon scattering mechanisms, increasing the number of heat-conducting chains and enhancing filler–PCM compatibility to address challenges in advancing PCC thermal conductivity.

C. The status of reducing the sunlight reflection

The change in the refractive index at the interface between smooth surfaces and air causes Fresnel reflection, resulting in high reflectivity of light.[53] For solar-thermal conversion PCC, the rough surface, covered with opaque PCM, effectively functions as a smooth surface where Fresnel reflection occurs. As a result, some of the incident light is transmitted into the PCM, while the rest is reflected, severely limiting light absorption. Although the addition of large quantities of 0D-3D fillers with high solar-thermal conversion efficiency, their flat configurations lead to considerable light reflection and reduced solar absorption, particularly for 2D fillers.[54]

The issue of light reflection in PCC can be mitigated by controlling the microscopic morphology.[54–58] The purpose of microscopic morphology control is to transform 2D light-absorbing interfaces into 3D structures. Energy efficiency in 2D planar structures is inherently constrained by diffuse reflection and thermal radiation. A carefully designed 3D light-capturing structure can change the direction of light propagation, thereby extending the internal light path. This leads to multiple refractions and reflections within the light-capturing microstructure, reducing energy loss from reflected light and improving light absorption, with only a small fraction of the incident light being reflected back to the sky.[59] Due to the limited research on reducing reflection in the existing solar-thermal PCC, this work highlights studies from other fields, particularly structural designs in solar interface evaporation (SIE). These insights are expected to provide inspiration for the structural design of solar-thermal PCC. The existing microstructures can be categorized into two types: microporous structures and biomimetic structures.

1. Porous structure

Various methods, including template, sol-gel, freeze-drying, and etching, are used to prepare porous materials.[49] The underlying principle is similar: dispersing fillers to form a 3D structure through interactions like van der Waals interactions. Nanosheets within the network can capture sunlight at different angles, with the porous structure extending the light path through multiple scattering, enhancing light collection efficiency.[60]

Aerogels, with over 80% porosity, low densities ($<100\ kg/m^3$), and high specific surface areas ($>800\ m^2/g$),[61] have excellent light absorption properties. Zhao *et al.*[62] used a co-gelation strategy to assemble 2D MXene sheets into 3D porous structures with small amounts of GO and ethylenediamine as a crosslinker. The MXene-GO composite enhances light absorption by extending the multi-reflected optical path, appearing darker than samples without MXene. Meng *et al.*[63] designed gradient vertical-channel aerogels from N-doped reduced graphene oxide (N-rGO) meshes, which reflect and scatter incident light multiple times. The ring-like composite reached a

maximum temperature of 97.9 °C with 5 mg/mL GO concentration and can capture light from all angles (360°).

Hydrogels, with a 3D network structure, offer adjustable porosity and flexibility. Zhu *et al.*[64] prepared a 3D porous hydrogel (DPFC) by dispersing rGO and silver in a PVA network. The micro-porous structure of DPFCAg-0.16, with 30–40 μm length and 10–20 μm width, enhances light absorption and photothermal performance. Li *et al.*[65] developed a vertically aligned A-RGO/MXene hybrid hydrogel using directional freezing, which featured aligned channels for seawater desalination and wastewater purification. The hydrogel achieved about 97% of light absorption, due to MXene's high absorption and multiple reflections within the channels.

2D photothermal membranes with thermal barriers and water transport channels have gained attention for their low energy consumption, compact size, and ease of operation. Fan *et al.*[66] incorporated PS microspheres into a polysulfone (PSf) membrane coated with rGO(rGO@PSf) to create complex light reflection, enhancing solar light absorption through multiple scattering. In contrast, the flat, dense rGO@PSf surface reflected sunlight directly. CB nanoparticles were added to improve light absorption and water wettability by forming a nanoscale rough structure, increasing the light absorption rate of the CB/rGO/PS@PSf film to 96.25%.

2. Biomimetic structures

Various micro-/nanostructures that decrease light reflection and benefit light absorption can be found in nature. Constructing various intricate and unique biomimetic micro-nanostructures can effectively enhance solar energy utilization efficiency.

The structure of a forest community can take advantage of sunlight efficiently. Specifically, the surface albedo of evergreen needleleaf forest is lower than that of planar grass. Peng *et al.*,[67] drawing inspiration from this concept, developed a forest-like laser-induced graphene (LIG) structure to minimize light reflection in 2D graphene. The forest-like LIG exhibited a reflection of approximately 1% across the 280–2500 nm wavelength range. Its structure resembled a boreal coniferous forest, where the interaction of incident light with the "tree," "leaves," and "branches" increased internal multiple light reflection and absorption.

Flower-like structures have a higher surface area than spherical particles and improve solar-thermal conversion efficiency. When incident light hits photothermal materials with flower-like microstructures, the petal layers capture and reflect light, enhancing absorption through multiple reflections within the 3D structure. Li *et al.*[68] supported this by introducing GNS@MoS_2-SR, where the integration of flower-like MoS_2 onto graphene's flat surface (3D-GNS@MoS_2) significantly improved optical absorption. The 3D structure facilitated repeated light reflections, reducing reflectivity and achieving nearly 70% light absorption in the visible-NIR region, compared to 50% for 2D-GNS@MoS_2-SR.

In the rainforest, competition for sunlight is intense, which has led to the evolution of unique strategies for light capture. Wang *et al.*[69] suggested that the fenestrated structure of Monstera leaves plays a key role in capturing sunlight under oblique and diffuse sunlight. To explore this, they designed artificial trees with various leaf shapes and layers. Their results showed that Monstera-inspired, leaf-shaped leaves were more effective under oblique incidence compared to elliptical leaves. The 3D hierarchical structure and leaf fenestration facilitated multiple light reflections between the leaves. Moreover, under oblique incidence (from 0° to 75°) and dappled sunlight, the evaporation rates of artificial trees with leaf fenestration are 1.08–1.26 and 1.34–2.78 times those of artificial trees without leaf fenestration and a 2D evaporator, respectively.

This section summarizes the causes, potential solutions, and related studies of reflection. Since the existing research on solar-thermal PCC has largely overlooked improvements in reflection reduction, this work has instead reviewed studies from the related fields, particularly SIE, hoping to provide insights for future solar-thermal PCC designs. The current research primarily transforms smooth 2D surfaces into rough 3D surfaces and incorporates various light-capturing structures. These designs enhance internal multiple refractions and reflections of incident light, compensating for the high reflectivity through repeated absorption. The existing structures can generally be categorized into porous structures and biomimetic structures, both of which achieve promising results. The best current result achieves a reflection of only about 1% within the 280–2500 nm wavelength range. Previous solar-thermal PCC surfaces were covered with opaque PCM. Future designs could consider incorporating specialized photo-thermal conversion structures on the sunlight-receiving surface to reduce reflection.

D. The status of weakening the heat loss

Currently, there is limited research on reducing heat loss in solar-thermal PCC. Therefore, this work can only outline potential future design strategies through theoretical analysis and studies from related fields. Taking SIE as an example, if the absorber is in direct contact with water without any thermal management design,[70] it is estimated that there would be approximately 7% radiative loss, 5% convective loss, and 43% conductive loss to the water. Radiation loss and convection loss to the ambient are crucial energy loss channel, especially for high-temperature PCC systems,

$$q_{rad} = \sigma_{SB}\left(\varepsilon_{abs} T_{abs}^4 - \varepsilon_{amb} T_{amb}^4\right), \quad (1)$$

$$q_{conv} = h(T_{abs} - T_{amb}), \quad (2)$$

where q_{rad} and q_{conv} represent the heat losses of the radiation and convection, respectively. σ_{SB} is the Stefan–Boltzmann constant. T_{abs} and T_{amb} are the temperature of absorber and the ambient, respectively. ε_{abs} and ε_{amb} are the thermal emissivity of absorber and the ambient, respectively. h is the convective coefficient, which depends on multiple factors, including the fluid properties, surface conditions, and other influencing variables. Ni *et al.*[71] was the first to employ a commercial spectrally selective absorber for suppressing radiation loss in SIE, with a high solar absorbance of 0.93 and a low thermal emissivity of 0.07. The result shows that the radiation loss can be suppressed by about one order of magnitude through selective absorbers.

Convection is more complicated than thermal conduction and radiation. There are many intrinsic and extrinsic factors that may influence the thermal convection (convection coefficient h) between the PCC and air: (1) geometric properties of the surface of the PCC, such as microstructure, surface roughness, and so on and (2) the flow properties of the air, natural or forced convection, the velocity of air, etc. It is challenging to study the reduction of convective heat transfer in isolation because it is difficult to precisely control the influence of various factors. Moreover, due to the presence of temperature

differences, since temperature difference is the driving force for heat transfer, radiation and convection occur simultaneously. Hence, up until now, there has been relatively little research related to thermal convection loss engineering. However, there are still some regularities to follow. As depicted in Eq. (2), one approach is to reduce the temperature difference between the PCC and the environment, which is closely related to the thermal conductivity discussed earlier. Another approach is to reduce the convective heat transfer coefficient. Ni *et al.*[71] covered the absorber with a sheet of large transparent bubble wrap, ensuring sunlight could penetrate while minimizing heat transfer between the absorber and the air. The result was a net improvement in the heat collection performance. Li *et al.*[6] reported a well-designed combined light-to-heat conversion layer incorporated with the PCC to reduce radiative and convective heat losses during the solar-thermal conversion process, aiming for direct high-temperature thermal energy harvest and storage with PCC. This synergistic effect enables the PCC to achieve sunlight-driven direct solar-thermal energy conversion and storage at temperatures exceeding 186 °C without optical concentration.

In this section, we analyzed the influencing factors of thermal losses and potential solutions, as illustrated in Fig. 2. In the current solar-thermal PCC research, there are limited focus on the suppression of thermal losses, so theoretical analysis can only be conducted from a heat transfer perspective to explore potential solutions. To reduce radiative heat loss, it is essential to lower the absorber temperature and use materials with low reflectivity. The suppression of convective heat transfer primarily involves reducing the convective heat transfer coefficient, which is influenced by many factors, and lowering the absorber temperature. How to reduce thermal losses remains a relatively underexplored and challenging area, requiring further in-depth research.

III. CONCLUSION AND PROSPECTS

As mentioned earlier, this work analyzes the heat transfer behavior in the solar-thermal conversion process. The results show that the absorption and heat conduction processes are beneficial and should be enhanced, while reflection and transmission (minor) in the first stage, along with thermal losses to the sky and air in the second stage, are unfavorable and need to be minimized. Most current research focuses on enhancing the beneficial processes, with less attention given to mitigating the unfavorable ones.

Efforts to improve solar-thermal absorption capacity through compositional adjustments have shown moderate success, as the theoretical limit (100%) restricts further breakthroughs. Special structures, like porous carbon spheres, extend heat-collecting surfaces beyond PCM, enhancing solar absorption through multiple reflections and achieving higher heat collection temperatures. Constructing additional structures under fixed composition ratios offers potential but remains underexplored.

To enhance thermal conductivity, oriented conduction pathways have proven effective, reaching a typical thermal conductivity of 33.5 W/(m·K) with filler loading below 25 wt. %, though still far below copper's 390 W/(m·K). Phonon scattering, mainly caused by interfacial thermal resistance between fillers and PCM, remains a key challenge. Grafting functional groups onto fillers improves compatibility and bonding strength; however, its application in solar-thermal PCC is limited. Future studies should focus on phonon mechanisms, heat-conducting chains, and filler–PCM interactions to enhance conductivity with minimal filler content.

Reflection suppression primarily involves transforming smooth 2D surfaces into rough 3D structures with light-capturing designs, enhancing multiple internal reflections and absorption. The current porous and biomimetic structures achieve promising results in the field of SIE, with the best achieving only 1% reflection in the 280–2500 nm range. Future designs may require a synergistic structural design that combines light absorption, reflection, and thermal loss management.

Reducing heat loss, particularly radiative and convective, remains underexplored. Potential solutions include lowering absorber temperatures and convective heat transfer coefficient, along with using low-reflectivity materials, but this area requires further in-depth study to address significant challenges.

As illustrated in Fig. 3, the design of high-efficiency solar-thermal PCC should continue to focus on the structural design, similar to the approach in the field of SIE. Ideally, a PCC is better designed as a multi-layer "sandwich" structure, consisting of a convective isolation layer, a heat collection layer, and a high conductivity PCC layer from top to bottom, with insulation measures on all sides. The convective

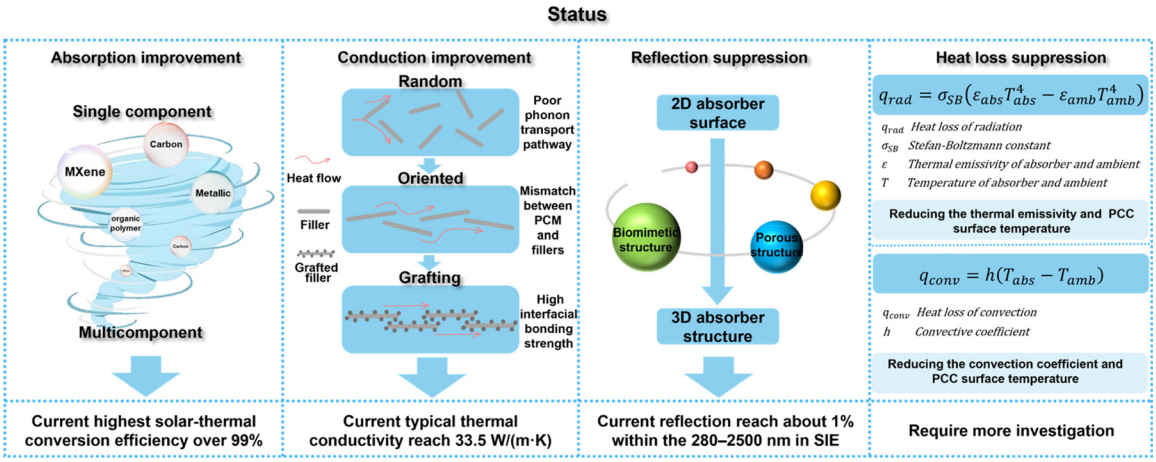

FIG. 2. Status of solar-thermal PCC in absorption, conduction, reflection, and heat loss.

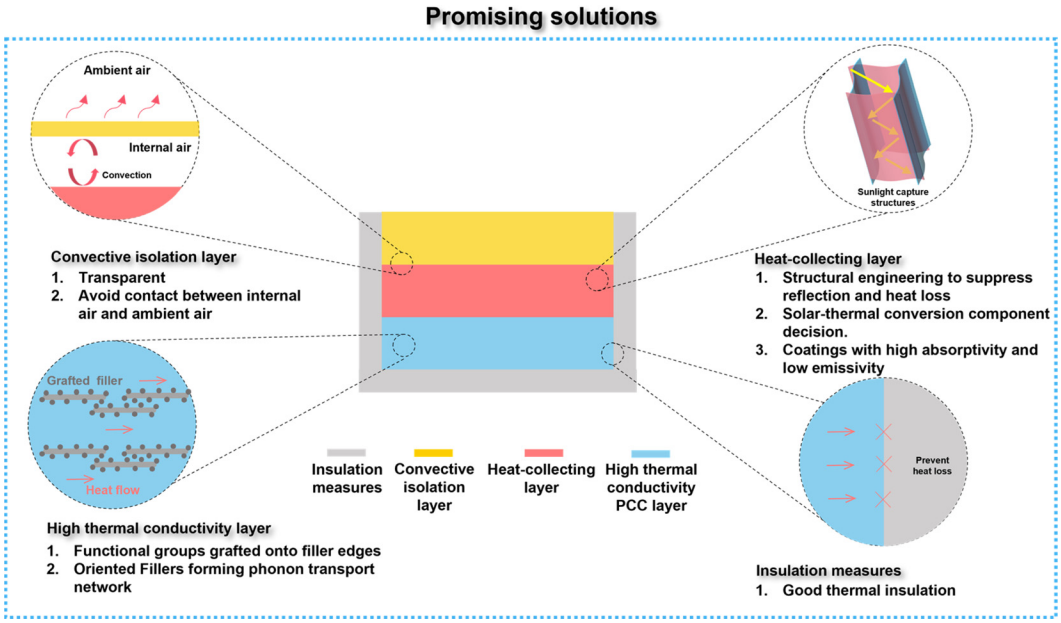

FIG. 3. Promising solutions for enhancing solar-thermal PCC.

isolation layer serves to prevent heat loss while not obstructing sunlight from reaching the heat collection layer. As the heat-collecting layer is not integrated with PCM, it can elevate the collected heat to medium temperatures, thus broadening its range of potential applications. The design of the heat collection layer should address the synergistic suppression of reflection, convection, and radiation, as well as the selection of heat collection materials. The high-conductivity PCM layer is designed with a large number of thermal conduction networks, allowing heat collected by the heat collection layer to be transferred to the PCM for storage, achieving high-efficiency solar-thermal conversion.

The vitality of a research field lies in its close integration with practical applications and its continuous exploration of new application directions. The application of solar-thermal PCC spans areas such as human thermal management, wearable devices, and home heating, especially with emerging prospects in seawater desalination and medium-temperature thermal energy storage. Addressing global water scarcity, integrating PCM with solar interfacial evaporation could enable nighttime desalination, increasing freshwater yield by extending operational hours. For medium-temperature (100–200 °C) industrial processes, which dominate energy consumption, solar-thermal PCC offers potential for carbon emission reduction. However, challenges remain in achieving high collection temperatures due to low solar power density and near-theoretical efficiency limits without optical concentration. Structural optimization may provide viable solutions, driving advancements in both seawater desalination and industrial thermal energy applications.

This study aims to guide and promote the development of solar-thermal PCC, enhancing the utilization of renewable solar energy and effectively addressing the challenges of energy crises and environmental pollution. In this work, the heat transfer behavior during the solar-thermal conversion process is analyzed, and four primary research directions are summarized: enhancing absorption, improving heat conduction, suppressing reflection, and reducing heat loss. Additionally, we analyzed the factors influencing thermal losses and explored potential solutions. Meanwhile, this study presents a comprehensive overview of the current advancements in solar-thermal regulation, with the goal of strengthening research efforts and accelerating the transition from the "fossil fuel era" to a sustainable "solar energy era."

ACKNOWLEDGMENTS

This work was supported by the National Natural Science Foundation of China (Grant Nos. 52436003 and U20A20299) and the Guangdong Basic and Applied Basic Research Foundation (Grant No. 2023A1515011985).

AUTHOR DECLARATIONS

Conflict of Interest

The authors have no conflicts to disclose.

Author Contributions

Zhizhao Mai and Kaijie You contributed equally to this work.

Zhizhao Mai: Investigation (equal); Writing – original draft (equal); Writing – review & editing (equal). **Kaijie You:** Investigation (equal); Writing – original draft (equal). **Jianyong Chen:** Investigation (equal). **Xinxin Sheng:** Conceptualization (lead); Funding acquisition (equal); Writing – review & editing (equal). **Ying Chen:** Funding acquisition (equal); Writing – review & editing (equal).

DATA AVAILABILITY

Data sharing is not applicable to this article as no new data were created or analyzed in this study.

REFERENCES

[1]X. Ke, X. Mu, S. Chen, Z. Zhang, J. Zhou, Y. Chen, J. Gao, J. Liu, X. Wang, C. Ma, and L. Miao, Soft Sci. **3**, 1 (2023).
[2]Y. Ma, J. Shen, T. Li, X. Sheng, and Y. Chen, Sol. Energy Mater. Sol. Cells **276**, 113078 (2024).
[3]T. Jia, J. Huang, R. Li, P. He, and Y. Dai, Renewable Sustainable Energy Rev. **90**, 475–489 (2018).
[4]L. Kumar, M. Hasanuzzaman, and N. A. Rahim, Energy Convers. Manage. **195**, 885–908 (2019).
[5]G. Alva, Y. Lin, and G. Fang, Energy **144**, 341–378 (2018).
[6]T. Li, M. Wu, S. Wu, S. Xiang, J. Xu, J. Chao, T. Yan, T. Deng, and R. Wang, Nano Energy **89**, 106338 (2021).
[7]J. C. C. Fan, F. J. Bachner, G. H. Foley, and P. M. Zavracky, Appl. Phys. Lett. **25**(12), 693–695 (1974).
[8]L. Shi, X. Wang, Y. Hu, Y. He, and Y. Yan, Appl. Therm. Eng. **179**, 115691 (2020).
[9]W. Aftab, A. Mahmood, W. Guo, M. Yousaf, H. Tabassum, X. Huang, Z. Liang, A. Cao, and R. Zou, Energy Storage Mater. **20**, 401–409 (2019).
[10]Y. Yue, X. Li, Z. Zhao, H. Wang, and X. Guo, Soft Sci. **3**, 13 (2023).
[11]H. He, Y. Wang, Z. Zhao, Q. Wang, Q. Wei, and Y. Cai, J. Energy Storage **55**, 105358 (2022).
[12]Q. Zhang and J. Liu, Sol. Energy Mater. Sol. Cells **190**, 1–5 (2019).
[13]J. Yang, L.-S. Tang, R.-Y. Bao, L. Bai, Z.-Y. Liu, W. Yang, B.-H. Xie, and M.-B. Yang, Chem. Eng. J. **315**, 481–490 (2017).
[14]A. R. Akhiani, H. S. Cornelis Metselaar, B. C. Ang, M. Mehrali, and M. Mehrali, Composites, Part B **264**, 110885 (2023).
[15]Y. Shao, W. Hu, M. Gao, Y. Xiao, T. Huang, N. Zhang, J. Yang, X. Qi, and Y. Wang, Composites, Part A **143**, 106291 (2021).
[16]H. Wang, Y. Deng, Y. Liu, F. Wu, W. Wang, H. Jin, J. Zheng, and J. Lei, Composites, Part A **155**, 106853 (2022).
[17]Y. Zhang, J. Wang, J. Qiu, X. Jin, M. M. Umair, R. Lu, S. Zhang, and B. Tang, Appl. Energy **237**, 83–90 (2019).
[18]R. Yan, Z. Huang, Y. Chen, L. Zhang, and X. Sheng, Int. J. Biol. Macromol. **277**, 134233 (2024).
[19]T. Wei, Y. Liu, W. Dong, Y. Zhang, C. Huang, Y. Sun, X. Chen, and N. Dai, ACS Appl. Mater. Interfaces **5**(21), 10473–10477 (2013).
[20]F. Xiong, K. Yuan, W. Aftab, H. Jiang, J. Shi, Z. Liang, S. Gao, R. Zhong, H. Wang, and R. Zou, ACS Appl. Mater. Interfaces **13**(1), 1377–1385 (2021).
[21]X. Fan, X. Qiu, L. Lu, and B. Zhou, Sol. Energy Mater. Sol. Cells **223**, 110937 (2021).
[22]L. Kong, Z. Wang, X. Kong, L. Wang, Z. Ji, X. Wang, and X. Zhang, ACS Appl. Mater. Interfaces **13**(25), 29965–29974 (2021).
[23]X. Du, J. Wang, L. Jin, S. Deng, Y. Dong, and S. Lin, ACS Appl. Mater. Interfaces **14**(13), 15225–15234 (2022).
[24]H. Wu, R. Chen, Y. Shao, X. Qi, J. Yang, and Y. Wang, ACS Sustainable Chem. Eng. **7**(15), 13532–13542 (2019).
[25]C. Liu, J. Zhang, J. Liu, Z. Tan, Y. Cao, X. Li, and Z. Rao, Angew. Chem. Int. Ed. **60**(25), 13978–13987 (2021).
[26]Y. Liu, H. Yang, Y. Wang, C. Ma, S. Luo, Z. Wu, Z. Zhang, W. Li, and S. Liu, Chem. Eng. J. **424**, 130426 (2021).
[27]X. Du, J. Qiu, S. Deng, Z. Du, X. Cheng, and H. Wang, ACS Appl. Mater. Interfaces **12**(5), 5695–5703 (2020).
[28]F. Wei, C.-P. Feng, J. Yang, L.-Y. Yang, L. Bai, R.-Y. Bao, Z.-Y. Liu, M.-B. Yang, and W. Yang, ACS Appl. Mater. Interfaces **13**(49), 59364–59372 (2021).
[29]R. Shen, M. Weng, L. Zhang, J. Huang, and X. Sheng, Composites, Part A **163**, 107248 (2022).
[30]L. Lv, Y. Wang, H. Ai, T. Chen, X. Zhang, and S. Song, J. Mater. Chem. A **10**(14), 7773–7784 (2022).
[31]J. Yang, G.-Q. Qi, R.-Y. Bao, K. Yi, M. Li, L. Peng, Z. Cai, M.-B. Yang, D. Wei, and W. Yang, Energy Storage Mater. **13**, 88–95 (2018).
[32]X. Chen, P. Cheng, Z. Tang, X. Xu, H. Gao, and G. Wang, Adv. Sci. **8**(9), 2001274 (2021).
[33]Y. Xiao, T. Li, Y. Yang, J. Lin, X. Sheng, J. Huang, T. Li, X. Lu, and D. Xie, Sol. Energy Mater. Sol. Cells **282**, 113369 (2025).
[34]G. Wang, Z. Tang, Y. Gao, P. Liu, Y. Li, A. Li, and X. Chen, Chem. Rev. **123**(11), 6953–7024 (2023).
[35]K. Sun, H. Dong, Y. Kou, H. Yang, H. Liu, Y. Li, and Q. Shi, Chem. Eng. J. **419**, 129637 (2021).
[36]X. He, C. Cui, Y. Chen, L. Zhang, X. Sheng, and D. Xie, Adv. Funct. Mater. **34**(51), 2409675 (2024).
[37]Z. Mo, P. Mo, M. Yi, Z. Hu, G. Tan, M. S. Selim, Y. Chen, X. Chen, Z. Hao, and X. Wei, Sol. Energy Mater. Sol. Cells **219**, 110813 (2021).
[38]P. Guo, D. Zhang, N. Sheng, Z. Rao, and C. Zhu, J. Energy Storage **80**, 110365 (2024).
[39]J. Lin, J. Huang, Z. Guo, B. Xu, Y. Cao, J. Ren, H. Hou, Y. Xiao, M. Elashiry, Z. El-Bahy, and Y. Min, Small **20**(46), 2402938 (2024).
[40]M. Liu, R. Qian, Y. Yang, X. Lu, L. Huang, and D. Zou, Adv. Funct. Mater. **34**(33), 2400038 (2024).
[41]S. Yuan, H. Wang, X. Li, Z. Du, X. Cheng, and X. Du, Composites, Part A **160**, 107048 (2022).
[42]Y. Chen, Y. Meng, J. Zhang, Y. Xie, H. Guo, M. He, X. Shi, Y. Mei, X. Sheng, and D. Xie, Nano-Micro Lett. **16**, 196 (2024).
[43]B. Kalidasan and A. K. Pandey, Prog. Mater. Sci. **148**, 101380 (2025).
[44]S. Wu, T. Yan, Z. Kuai, and W. Pan, Energy Storage Mater. **25**, 251–295 (2020).
[45]L. Wang, H. Yu, and W. Feng, Research **7**, 0460 (2024).
[46]Q. Yan, F. E. Alam, J. Gao, W. Dai, X. Tan, L. Lv, J. Wang, H. Zhang, D. Chen, K. Nishimura, L. Wang, J. Yu, J. Lu, R. Sun, R. Xiang, S. Maruyama, H. Zhang, S. Wu, N. Jiang, and C. Lin, Adv. Funct. Mater. **31**(36), 2104062 (2021).
[47]H. Jiang, J. Li, Y. Xie, H. Guo, M. He, X. Shi, Y. Mei, X. Sheng, and D. Xie, J. Mater. Sci. Technol. **209**, 207–218 (2025).
[48]J. Gao, Q. Yan, L. Lv, X. Tan, J. Ying, K. Yang, J. Yu, S. Du, Q. Wei, R. Xiang, Y. Yao, X. Zeng, R. Sun, C.-P. Wong, N. Jiang, C.-T. Lin, and W. Dai, Chem. Eng. J. **419**, 129609 (2021).
[49]J. Bian, L. Liao, and G. Lv, J. Energy Storage **102**, 114155 (2024).
[50]Q. Yan, W. Dai, J. Gao, X. Tan, L. Lv, J. Ying, X. Lu, J. Lu, Y. Yao, Q. Wei, R. Sun, J. Yu, N. Jiang, D. Chen, C.-P. Wong, R. Xiang, S. Maruyama, and C.-T. Lin, ACS Nano **15**(4), 6489–6498 (2021).
[51]N. Hu, H. Li, Q. Wei, K. Zhou, W. Zhu, L. Zhang, S. Li, W. Ye, Z. Jiao, J. Luo, L. Ma, Q. Yan, and C.-T. Lin, Composites, Part B **200**, 108293 (2020).
[52]M. Li, M. Chen, Z. Wu, and J. Liu, Energy Convers. Manage. **83**, 325–329 (2014).
[53]H. Xie, W. Xu, Y. Du, J. Gong, R. Niu, T. Wu, and J. Qu, Small **18**(17), 2200175 (2022).
[54]I. Ibrahim, D. H. Seo, A. M. McDonagh, H. K. Shon, and L. Tijing, Desalination **500**, 114853 (2021).
[55]T. Jiang, S. Bian, Y. Wang, X. Fan, L. Zhu, X. Song, G. Wang, T. Wang, and H. Zhang, Chem. Eng. J. **499**, 156450 (2024).
[56]A. C. Da Silva, T. E. Paterson, and I. R. Minev, Soft Sci. **3**, 3 (2023).
[57]Y. Shi, R. Li, Y. Jin, S. Zhuo, L. Shi, J. Chang, S. Hong, K.-C. Ng, and P. Wang, Joule **2**(6), 1171–1186 (2018).
[58]L. Zhu, L. Tian, S. Jiang, L. Han, Y. Liang, Q. Li, and S. Chen, Chem. Soc. Rev. **52**(21), 7389–7460 (2023).
[59]Y. Zhang, T. Xiong, D. K. Nandakumar, and S. C. Tan, Adv. Sci. **7**(9), 1903478 (2020).
[60]Q. Zhou, H. Li, D. Li, B. Wang, H. Wang, J. Bai, S. Ma, and G. Wang, J. Colloid Interface Sci. **592**, 77–86 (2021).
[61]F. Lou, S. Dong, K. Zhu, X. Chen, and Y. Ma, Gels **9**(3), 220 (2023).
[62]X. Zhao, L.-M. Peng, C.-Y. Tang, J.-H. Pu, X.-J. Zha, K. Ke, R.-Y. Bao, M.-B. Yang, and W. Yang, Mater. Horiz. **7**(3), 855–865 (2020).
[63]X. Meng, J. Yang, S. Ramakrishna, Y. Sun, and Y. Dai, ACS Sustainable Chem. Eng. **8**(12), 4955–4965 (2020).
[64]L. Zhu, J. Li, L. Zhong, L. Zhang, M. Zhou, H. Chen, Y. Hou, and Y. Zheng, Nano Energy **100**, 107441 (2022).
[65]W. Li, X. Li, W. Chang, J. Wu, P. Liu, J. Wang, X. Yao, and Z.-Z. Yu, Nano Res. **13**(11), 3048–3056 (2020).
[66]H. Fan, A. Gao, G. Zhang, S. Zhao, J. Cui, and Y. Yan, Chem. Eng. J. **415**, 128798 (2021).
[67]Y. Peng, W. Zhao, F. Ni, W. Yu, and X. Liu, ACS Nano **15**(12), 19490–19502 (2021).
[68]S. Song, Z. Xing, K. Wang, H. Zhao, P. Chen, Z. Li, and W. Zhou, Green Energy Environ. **8**(1), 200–212 (2023).
[69]H. Wang, C. Zhang, Z. Zhang, B. Zhou, J. Shen, and A. Du, Adv. Funct. Mater. **30**(48), 2005513 (2020).
[70]X. Li, R. Lin, G. Ni, N. Xu, X. Hu, B. Zhu, G. Lv, J. Li, S. Zhu, and J. Zhu, Natl. Sci. Rev. **5**(1), 70–77 (2018).
[71]G. Ni, G. Li, S. V. Boriskina, H. Li, W. Yang, T. Zhang, and G. Chen, Nat. Energy **1**(9), 16126 (2016).